

September 2010

SUSTAINABLE RECOVERY OF POTABLE WATER FROM SALINE WATERS

WRRRI Technical Completion Report No. 355

N. Nirmala Khandan
Veera Gnaneswar Gude



NEW MEXICO WATER RESOURCES RESEARCH INSTITUTE
New Mexico State University
MSC 3167, Box 30001
Las Cruces, New Mexico 88003-0001
Telephone (575) 646-4337 FAX (575) 646-6418
email: nmwrri@wrrri.nmsu.edu

SUSTAINABLE RECOVERY OF POTABLE WATER FROM SALINE WATERS

By

N. Nirmala Khandan
Principal Investigator
Civil Engineering Department
New Mexico State University

Veera Gnaneswar Gude
Graduate Research Assistant
Civil Engineering Department
New Mexico State University

TECHNICAL COMPLETION REPORT

Index Number: 109467

September 2010

New Mexico Water Resources Research Institute

in cooperation with

Civil Engineering Department
New Mexico State University

The research on which this report is made was financed in part by the U.S. Department of the Interior, Geological Survey, through New Mexico Water Resources Research Institute.

Disclaimer

The purpose of the Water Resources Research Institute (WRI) technical reports is to provide a timely outlet for research results obtained on projects supported in whole or part by the institute. Through these reports the WRI promotes the free exchange of information and ideas and hopes to stimulate thoughtful discussions and actions that may lead to resolution of water problems. The WRI, through peer review of draft reports, attempts to substantiate the accuracy of information contained within its reports, but the views expressed are those of the authors and do not necessarily reflect those of the WRI or its reviewers. Contents of this publication do not necessarily reflect the views and policies of the Department of the Interior, nor does the mention of trade names or commercial products constitute their endorsement by the United States government.

Abstract

A new low-temperature phase change desalination process capable of being driven by low-grade or waste heat sources was developed and demonstrated at prototype scale. The proposed process is based on simple but sound scientific principles, and has the potential to produce potable-quality water in a sustainable manner, without any reliance on grid power. In this project, theoretical experimental studies were conducted to characterize and demonstrate the feasibility of the process. Based on theoretical simulations, a typical absorption refrigeration system driven by a 25 m² solar collector and rated at a cooling rate of 3.25 kW (0.975 tons of refrigeration for typical domestic application) can produce 4.5 kg/h (108 L/d) of desalinated water. The net grid energy required for this case was 208 kJ/kg of desalinated water. The feasibility of an alternate configuration that could be driven solely by solar energy incorporating solar photovoltaic panel and a battery bank was demonstrated at prototype scale. Results of this study showed that a freshwater production rate of 0.25 kg/h (6 L/d) can be sustained at evaporation temperatures as low as 40°C using a solar PV panel of area 6 m². The study also demonstrated that the system was able to produce EPA-recommended potable-quality water from the effluent of a municipal wastewater treatment plant, with the following removal efficiencies of key contaminants: > 93% total dissolved solids; >95% nitrates; > 97% ammonia; and > 99.9% coliform bacteria. Since this process can be driven entirely by renewable or waste energy, unlike the traditional desalination processes, it does not contribute to any greenhouse gas emissions.

Table of Contents

1.0	Introduction	1
2.0	Proposed desalination system.....	1
2.1	Thermodynamic rationale for low temperature desalination	1
2.2	Process configuration.....	4
3.0	Results and discussion.....	6
3.1	Desalination system driven by waste heat	6
3.1.1	Analysis of ARS.....	8
3.1.2	Volume of TES tank.....	8
3.1.3	Solar collector for ARS	9
3.1.4	Energy requirements.....	10
3.1.5	Brine withdrawal vs. system performance	10
3.2	Desalination system driven by solar photovoltaic/battery system.....	11
3.2.1	Using direct solar energy.....	12
3.2.2	Using PV panel and direct solar energy	14
3.3	Reclamation of wastewater treatment plant effluent	18
4.0	Conclusions	19
5.0	Acknowledgements	19
6.0	References	20

List of Figures

Figure 1.	Generic representation of a phase-change desalination process	2
Figure 2.	Contours of freshwater production rate as a function of saline water feed rate and evaporation temperature at fixed heat input of 1,000 kJ/hr	3
Figure 3.	Relationship between yield and specific energy consumption as a function of evaporation temperature.....	3
Figure 4.	Schematic arrangement of the proposed system	4
Figure 5.	Photographs of the prototype system designed and built in this project	5
Figure 6.	Schematic of the desalination system driven by an absorption refrigeration system	6
Figure 7.	Rates of heat exchanges and efficiency over 24 hours.....	7
Figure 8.	Evaporation chamber, freshwater, and ambient temperature variations over 24 hours	8
Figure 9.	Ambient and TES temperature variations over 24 hours	9
Figure 10.	Solar fraction and optimum solar fraction area	9
Figure 11.	Desalination rates at different cooling rates and solar panel areas.....	10
Figure 12.	Relationship between withdrawal rate, efficiency and temperature of EC	11
Figure 13.	Schematic of the configuration (b): use of solar PV panel/battery bank.....	11
Figure 14.	Typical temperature profiles in configuration (a) over 1-day period	12
Figure 15.	Daily distillate production in configuration (a): Measured vs. predicted.....	13
Figure 16.	Distillation efficiency in configuration (a): Measured vs. predicted.....	13
Figure 17.	Distillate production with and without a reflector in configuration (a)	14
Figure 18.	Energy flows in configuration (b) over a typical 1-day period	15
Figure 19.	Temperature profiles in configuration (b) with PV/battery.....	16
Figure 20.	Energy produced, energy consumed, and excess energy	16
Figure 21.	Distillate production in configuration (b) with PV/battery	17

List of Tables

Table I.	ARS system parameters: typical values versus and values in this study.....	8
Table II.	Comparison of proposed process with traditional desalination processes	17
Table III.	Water quality measures before and after treatment.....	18

Sustainable Recovery of Potable Water from Saline Waters

1.0 Introduction

Increasing demand for water due to population explosion and rapid industrialization is a major concern locally, nationally, and worldwide. This problem is compounded further by dwindling water sources of appropriate quantity and quality and their impairment by natural and man-made pollution. Adding to this problem are the energy requirements of current technologies to restore impaired sources, the adverse environmental impacts of these technologies, and the limited energy sources that can provide the required energy. In addition, production of energy to meet water demands in itself requires water. Since water is essential to continued existence of life, it is obviously critical to develop sustainable technologies to ensure that water demands of future generations will be met using renewable resources with minimal impacts on the environment.

Even though water is one of the most abundant resources, covering three-fourths of the planet's surface, about 97% of this volume is saline, and only 3% is fresh water suitable for humans, plants, and animals. The amount of water in the oceans can serve as an inexhaustible source for the planet's freshwater needs, if clean and sustainable technologies can be developed for desalination. Such technologies can also be adapted in several inland areas where large reservoirs of brackish water are readily available. The goal of this project was to build upon current research and incorporate several refinements to develop and demonstrate the feasibility of a new solar desalination system to produce high quality water from impaired waters such as seawater, brackish water, wastewaters and so on.

2.0 Proposed desalination system

The principles behind the proposed process can be illustrated by considering two barometric columns at ambient temperature, one with freshwater and one with saline water. The head space of these two columns will be occupied by the vapors of the respective fluids at their respective vapor pressures. Suppose these head spaces are connected to one another. Since the vapor pressure of freshwater is slightly higher than that of saline water at ambient temperature, water vapor will distill from the freshwater column into the saline water column.

However, if the temperature of the saline water column is maintained slightly higher than that of the fresh water column to raise the vapor pressure of the saline water side above that of the fresh water side, water vapor from the saline water column will distill into the fresh water column. A temperature differential of about 15°C is adequate to overcome the vapor pressure differential to drive this distillation process. Such low temperature differentials can be achieved using low-grade heat sources such as solar energy, waste process heat, or thermal energy storage systems.

2.1 Thermodynamic rationale for low temperature desalination

Desalination processes are energy intensive and the quality of energy used by the different processes can be quite diverse. For example, the reverse osmosis process uses mechanical energy; distillation uses high quality thermal energy; vacuum distillation utilizes mechanical and medium grade heat energy; and solar distillation technologies use low-grade heat energy. Phase-change desalination technologies have traditionally been analyzed and compared on the basis of the first law of thermodynamics, considering only the quantity of energy.

The generic phase-change desalination process is shown in Figure 1, where h is the specific enthalpy, T is the temperature, and Q is the heat transfer rate.

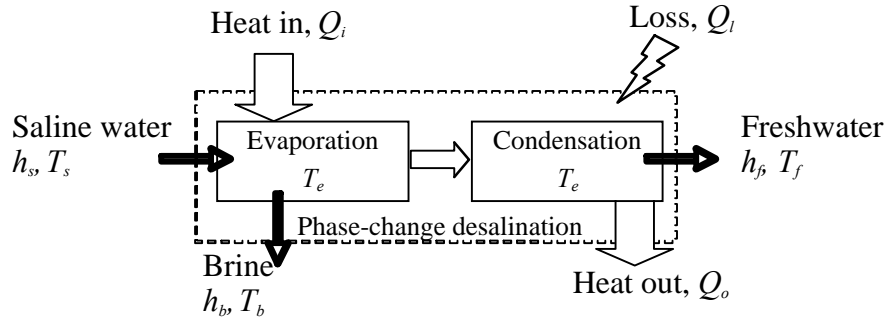


Figure 1. Generic representation of a phase-change desalination process

Here, $Q_o = m_f h_{L(T_e)}$ is the heat rejection rate, where m_f is the freshwater production rate and $h_{L(T_e)}$ is the latent heat of condensation at the evaporation temperature, T_e ; and $Q_l = UA\Delta T$ is the heat loss rate, where U is the heat transfer coefficient, A is the heat transfer area, and ΔT is the temperature difference between the evaporation chamber and the ambient. Based on the first law of thermodynamics, the yield of this process, m_f/m_s , can be shown to be:

$$\frac{m_f}{m_s} = \frac{(Q_i - Q_l)/m_s + (h_s - h_b)}{h_{L(T_e)} + h_f - h_b} \quad (1)$$

Using the above result, contours of freshwater production rate as a function of saline water feed rate and evaporation temperature can be generated for a given energy input. The results shown in Figure 2 for a Q_i of 1,000 kJ/hr and $UA = 0.8$ J/s-K indicate that for a given feed rate, higher production rate is possible at lower temperature. The relationship between the process yield, m_f/m_s , and the specific energy consumption, Q_i/m_f [kJ/kg of freshwater produced] at various evaporation temperatures is shown in Figure 3. This plot shows that the lower the evaporation temperature, the lower the specific energy requirement for a desired yield.

For rational technical comparisons of the different processes, and to improve existing processes or to develop new processes, the quality of the energy utilized should be considered as well. A simple second law-based evaluation is presented below to illustrate how different qualities of heat energy used in phase-change desalination processes can be compared. Consider, for example, the following two cases, each fed with saline water at 1 kg/hr:

- Case 1: a phase-change desalination process using moderate quality heat energy of 1,000 kJ/hr at an evaporation temperature of 90°C and ambient temperature of 25°C
- Case 2: a phase-change desalination process using low quality heat energy of 1,000 kJ/hr at an evaporation temperature of 50°C and ambient temperature of 25°C

Based on first law analysis, freshwater production rates in Cases 1 and 2 can be found as 0.294 kg/hr and 0.368 kg/hr, respectively (Figure 2); and, the corresponding specific energy requirements as 3,401 kJ/kg and 2,717 kJ/kg (Figure 3). Even though the quantities of energy input are the same in the two cases, their qualities are not. If for instance, an ideal heat engine is operated across the respective temperature differences, their Carnot efficiencies will be 20% and 7.7%, respectively. Thus, for the given heat energy input of 1,000 kW, the reversible work equivalence in Case 1 will be 201 kW and that in Case 2 will be 77 kW. On the basis of

reversible work equivalences, the specific energy requirements for the two cases will be 683 kJ/kg and 209 kJ/kg, respectively.

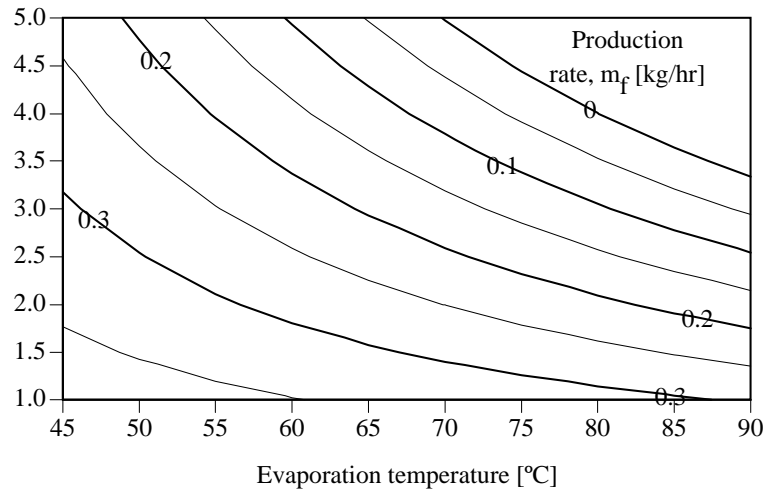


Figure 2. Contours of freshwater production rate as a function of saline water feed rate and evaporation temperature at fixed heat input of 1,000 kJ/hr

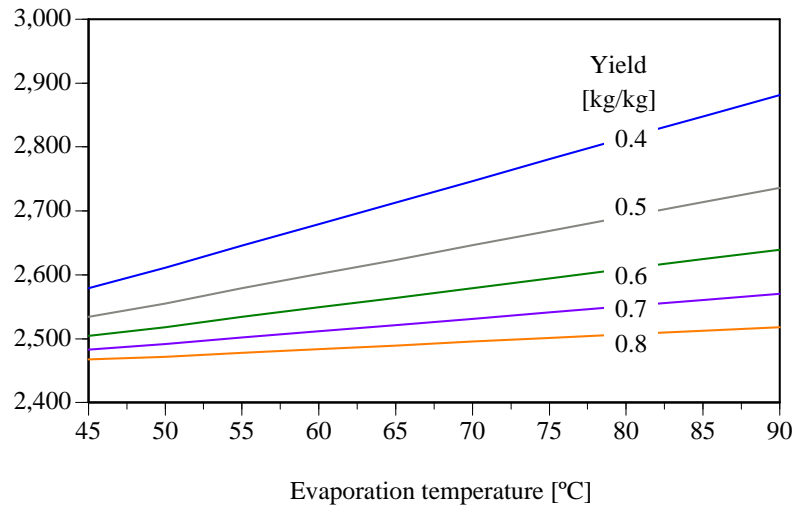


Figure 3. Relationship between yield and specific energy consumption as a function of evaporation temperature

While the above analyses indicate that the phase-change process can be more energy efficient at low temperatures, only a limited number of technologies have been engineered to take advantage of this result. One approach has been to decrease the overall temperature range of the external heat addition process by *staging*, where the heat rejected during the condensation step is recovered to preheat the feed. Another approach is to maintain a low evaporation pressure, whereby evaporation occurs at low temperature as in the case of vacuum distillation. In the latter case, additional mechanical energy has to be expended to maintain the required vacuum; since

mechanical energy is a more valuable form of energy than heat energy, it is not a thermodynamically efficient approach.

In addition to the thermodynamic advantage, operation of phase-change processes at low temperatures can be beneficial in several other ways (Gustavo & Fredi, 2001). Low corrosion rates at low temperatures allow low-cost materials to be used in construction and increases plant life. The scaling rate is minimal because the operating temperatures are well below saturation limits for most scalants. Low temperature operation reduces fugitive heat losses and start-up periods. The motive energy for driving low temperature processes can be provided by low-grade heat sources or waste heat rejections, so that overall economies can be achieved.

2.2 Process configuration

A schematic arrangement of the desalination system based on the above principles is shown in Figure 4. Components of the desalination unit include an evaporation chamber (EC), a natural draft condenser (CON), two heat exchangers (HE1 and HE2), and three 10-m tall columns. These three columns serve as the saline water column; the brine withdrawal column; and the freshwater column, each with its own constant-level holding tank, SWT, BT, and FWT, respectively. These holding tanks are installed at ground level while the EC is installed atop the saline water and brine withdrawal columns at the barometric height of about 10 m above the free surface in the holding tanks to create a Torricelli's vacuum in the head space of the EC. The top of the freshwater column is connected to the outlet of the condenser. When the temperature of the saline water in the EC is increased by about 20°C above the ambient temperature, water vapor will flow from the EC to the CON where it will condense and flow into the freshwater column. By maintaining constant levels in the holding tanks with suitable withdrawal rates of brine and distilled water, this configuration enables the desalination process to be run without any mechanical energy input for fluid transfer or holding the vacuum (Bemporad, 1995; Al-Kharabsheh, and Goswami, 2003a, b). The purpose of the heat exchanger HE1 is to preheat the saline water entering the EC by the brine stream withdrawn from the EC. The purpose of the heat exchanger HE2 is to provide the heat energy to the EC; any low-grade heat source can be utilized to provide this heat energy.

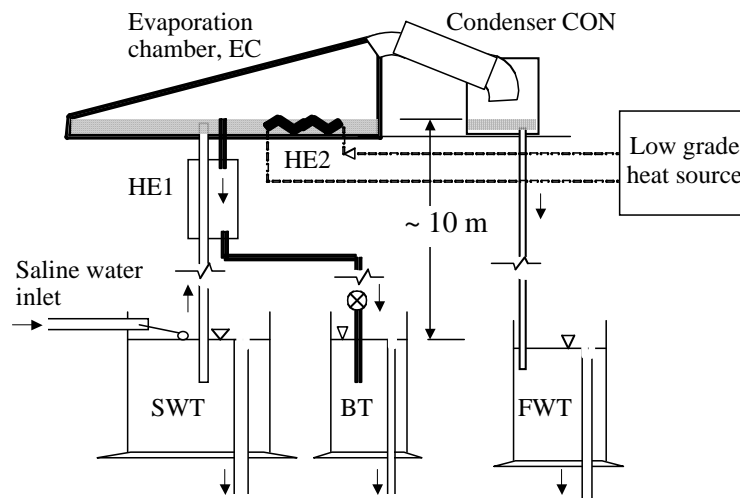


Figure 4. Schematic arrangement of the proposed system

In this project, the feasibility of utilizing two different primary heat sources was evaluated: a) low-grade heat rejected by an absorption refrigeration system (theoretical) and b) solar PV panel-battery system (theoretical and experimental). Two different feeds were evaluated experimentally at prototype scale: a) synthetic saline water and b) effluent from the Las Cruces Municipal Wastewater Treatment Plant.

The prototype scale system tested in this study (Figure 5) had an evaporator area of 1.0 m^2 and photovoltaic panel area of 6 m^2 . The heat energy required to maintain the evaporation chamber at the desired temperature was provided by a 12-V/18-W DC heater, which was powered by a bank of batteries. The batteries were charged by photovoltaic panel. Ambient temperature was measured by a thermocouple with an accuracy of $\pm 0.2\%$. Evaporation chamber temperature was set at various values and was measured by a thermocouple with an accuracy of $\pm 0.2\%$. Evaporation chamber pressure and condenser pressure were measured using pressure transducers with an accuracy of $\pm 0.3\%$. The power consumption was calculated from voltage and current measurements. A Campbell scientific data logger recorded the process data at ten-minute intervals. The depth of water in the evaporation chamber was fixed at 0.05 m. A rain gauge sensor with an accuracy of $\pm 1\%$ was used to measure freshwater production rate.

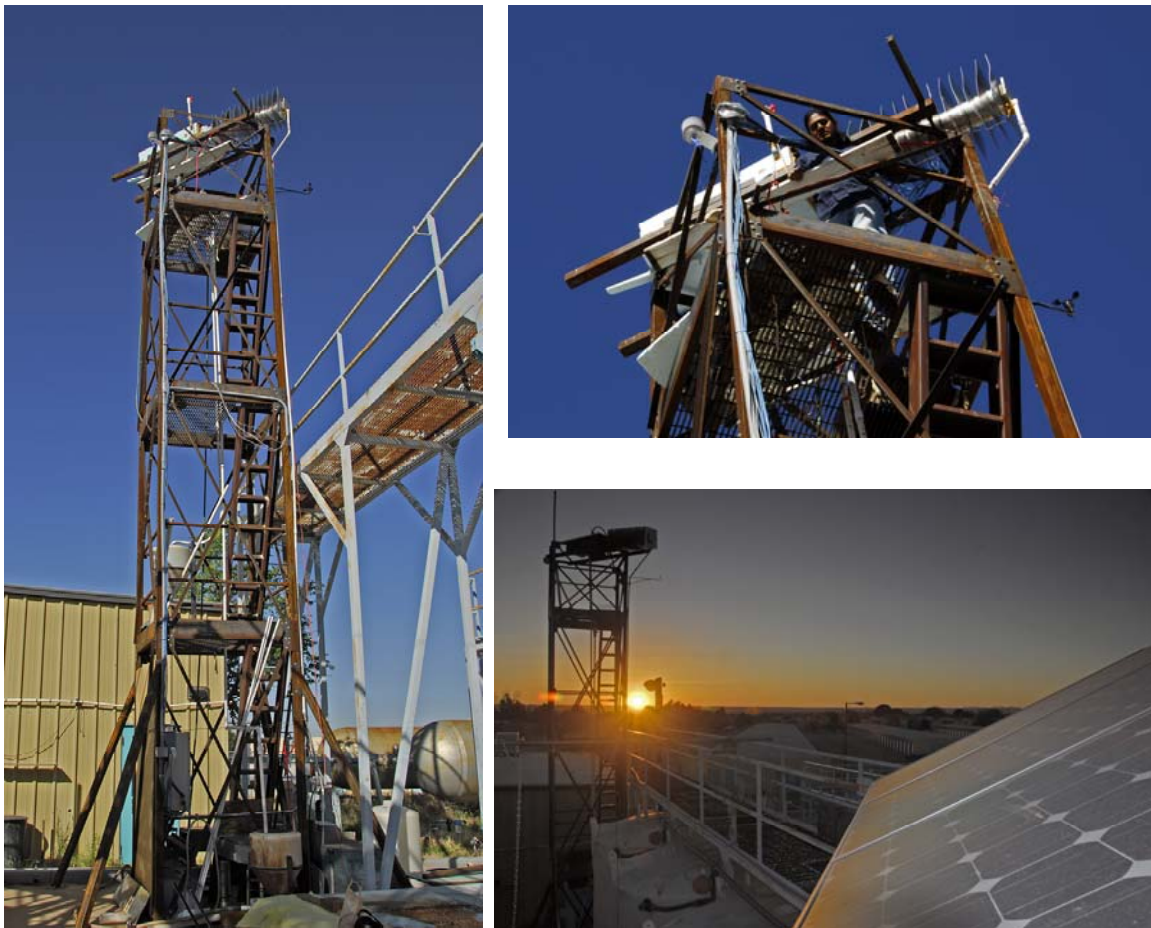


Figure 5. Photographs of the prototype system designed and built in this project

3.0 Results and Discussion

Under this grant, the system was first analyzed theoretically and process models were developed to characterize the performance of the system. Based on the theoretical analyses, a prototype system was designed and tested under different conditions with solar energy as the energy source. Details of the theoretical analyses have been presented in a PhD dissertation (Gude, 2007) and three peer-reviewed journal publications (Gude & Nirmalakhandan, 2008a; Gude & Nirmalakhandan, 2008b; Gude & Nirmalakhandan, 2009). In this report, detailed results from selected theoretical and experimental studies are presented.

3.1 Desalination driven by waste heat from an absorption refrigeration system

In this analysis, the feasibility of driving the desalination process using the heat rejected by an absorption refrigeration system (ARS) was evaluated theoretically. The process schematic for this configuration is shown in Figure 6. In this case, the EC is heated by a thermal energy storage (TES) system, which stored the heat rejected by the ARS. The ARS evaluated in this study operated with LiBr-H₂O as refrigerant under a pressure range of 1 to 16 kPa. Energy required to heat the generator of ARS is supplied by a solar collector during sunlight hours and by an auxiliary electric heater during non-sunlight hours.

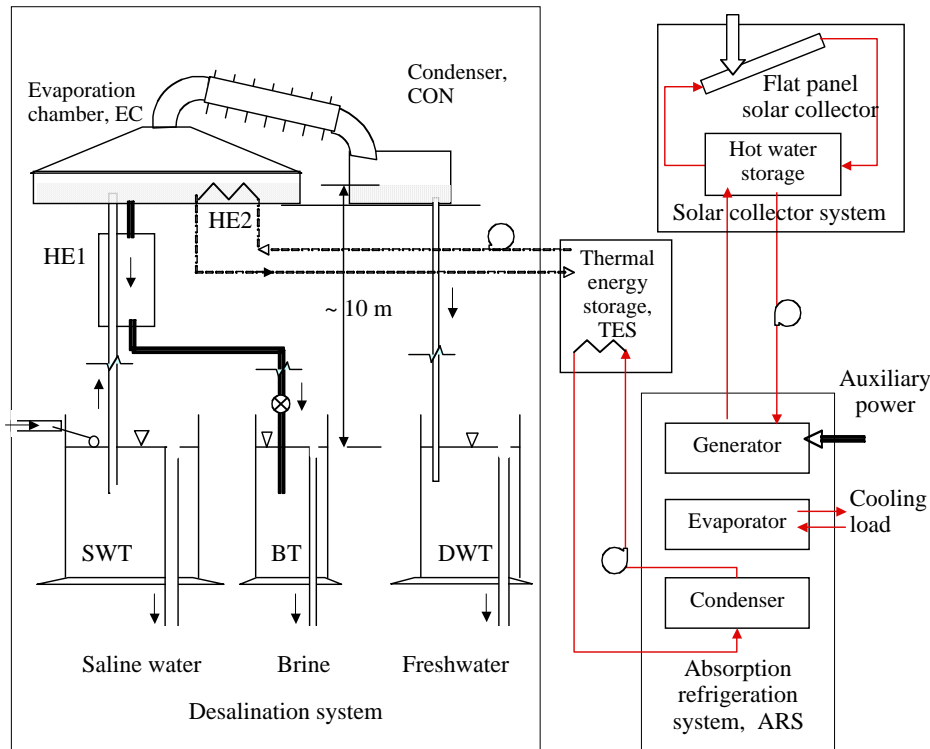


Figure 6. Schematic of the desalination system driven by an absorption refrigeration system

In this manner, the thermal energy to drive the desalination process is available round the clock. The generator of the ARS is maintained at 100°C. Since the evaporator of the ARS feeds the cooling load, the proposed system performs two functions of continuous desalination and cooling with a reduced amount of external non-renewable energy input. The ARS is sized to maintain the TES at 50°C.

A process model for the above system has been developed based on mass and energy balances and solved using Extend[®] and EES[®] simulation software packages (Gude 2007). An evaporator area of 5 m² and a height of 0.25 m were considered. In all calculations, the reference temperature used is 25°C. All heat exchangers were assumed to have 80% efficiency.

Major objective of the modeling exercise was to verify that a properly sized TES would be able to provide the required thermal energy to the evaporator to maintain the desalination rate over a 24-hr period. Figure 7 shows the variation in rates of heat supplied by the TES, the heat consumed for evaporation, and the heat lost over a 24-hr period for a summer day, when the ambient temperature ranged from 25 to 35°C. The desalination efficiency is also plotted in Figure 7. As expected, the energy lost by the EC is higher during non-sunlight hours than that during sunlight hours due to lower ambient temperatures during non-sunlight hours.

Under the base case conditions, the energy available for desalination is about 12,500 kJ/hr (= 3.45 kW), which is the waste heat rejected by the condenser in ARS. However, the net heat transfer is dependent on the temperature gradient between the transfer medium and the heat source. The actual mass of water that can be evaporated in the EC and hence, the desalination efficiency, will depend on the heat input rate from the TES, the ambient temperature at which the condensation takes place, and the brine withdrawal rate, as discussed later. Since the driving force for evaporation is the temperature difference between the EC and the condenser, the heat input to EC during the day is lower than that input during the night. During the night, the ambient temperature is low and the freshwater temperature is also low, which favors a higher desalination rate, thus resulting in a higher heat input and vice versa.

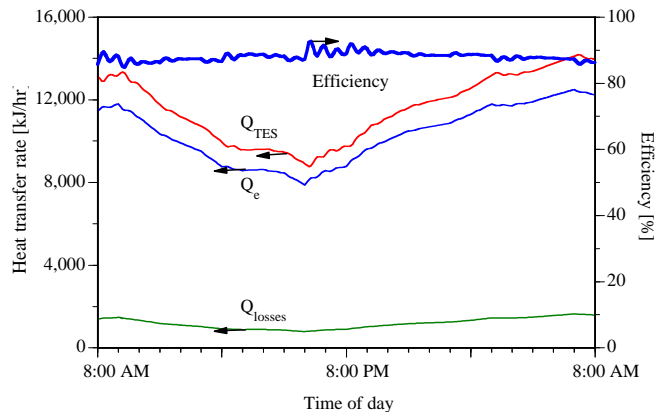


Figure 7. Rates of heat exchanges and efficiency over 24 hours

The variations in the saline water temperature in the EC and the fresh water temperatures with respect to ambient temperature are shown in Figure 8. The temperature of saline water varied from 43.5 to 46°C and the ambient temperature ranged from 25 to 37°C while the fresh water temperatures ranged from 35 to 40°C. From Figures 7 and 8, it is concluded that the TES is able to maintain the desalination efficiency and the temperature of the evaporation chamber at the desired operating conditions. As can be seen from these plots, ambient temperature is an important variable because condensation occurs at the ambient temperature, which indirectly determines the desalination rate in this process.

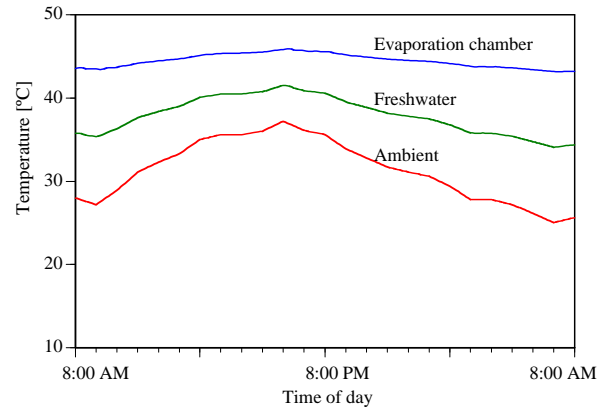


Figure 8. Evaporation chamber, freshwater, and ambient temperature variations over 24 hours

3.1.1 Analysis of ARS

The ARS configuration employed in the proposed system is designed for two functions – for maintaining the TES at the desired temperature and for providing the cooling load. As such, the proposed ARS operates under slightly different conditions compared to the traditional systems used for cooling alone. Operating conditions for typical ARS used in cooling and those for the ARS proposed in this study are compared in Table I, for the same cooling load of 3.25 kW. The notable difference is the pressure ranges – about 1 to 6 kPa versus 1.5 to 15.75 kPa, respectively. This is necessary to run the condenser at 55°C to maintain the TES at 50°C.

Table I. ARS system parameters: typical values versus and values in this study

Parameter	Typical value	This study
Absorber temperature (°C)	30	28
Condenser temperature (°C)	35	55
Evaporator temperature (°C)	8	12
Generator temperature (°C)	100	100
Condenser/Generator pressure (kPa)	6.27	15.75
Absorber/Evaporator pressure (kPa)	1.073	1.403
Energy transfer rate at absorber (kW)	4.32	4.43
Energy transfer rate at condenser (kW)	3.49	3.49
Energy transfer rate at evaporator (kW)	3.25	3.25
Energy transfer rate at generator (kW)	4.43	4.67
Coefficient of performance, COP (-)	0.73	0.72

3.1.2 Volume of TES tank

Winter conditions were assumed to determine the size of the TES necessary to provide the heat energy to the EC. This volume was found by solving the model equations (Gude 2007) by trial

and error so that the temperatures at the beginning and the end of a 24-hr period would be within $\pm 0.1^\circ\text{C}$. A tank volume of 10 m^3 was found to be adequate to maintain a temperature of 50°C throughout a 24-hr period and to provide the energy needs of the EC. Figure 9 shows that the TES temperature remained constant at the set value of 50°C while the ambient winter temperature ranged from 2 to 15°C .

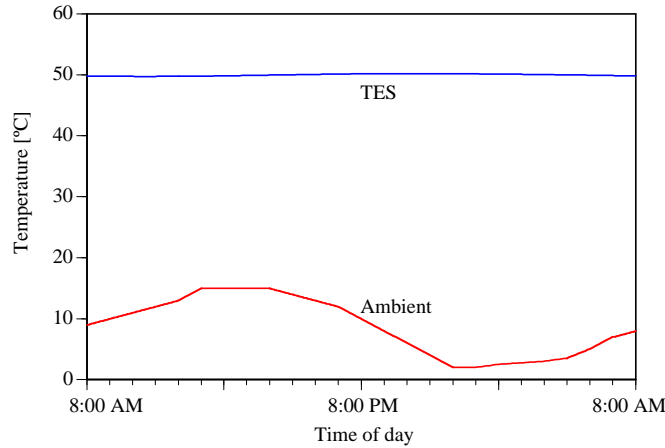


Figure 9. Ambient and TES temperature variations over 24 hours

3.1.3 Solar collector for ARS.

The solar collector, augmented by an auxiliary heater, is to be sized to provide for the TES and the cooling load. The desired temperature of the storage tank of the solar collector is set to 110°C in order to maintain the generator temperature at 100°C . The energy to be provided by the auxiliary heater is equal to the difference between the energy required by the generator and that can be collected from solar insolation. Figure 10 illustrates this difference and the solar fraction over a 24-hr period. For the base case considered here, solar collector area of 25 m^2 can satisfy a cooling load of 3.25 kW at an average desalination rate of 4.3 kg/hr . The relationships between desalination rate, solar panel area, and cooling load are presented in Figure 11.

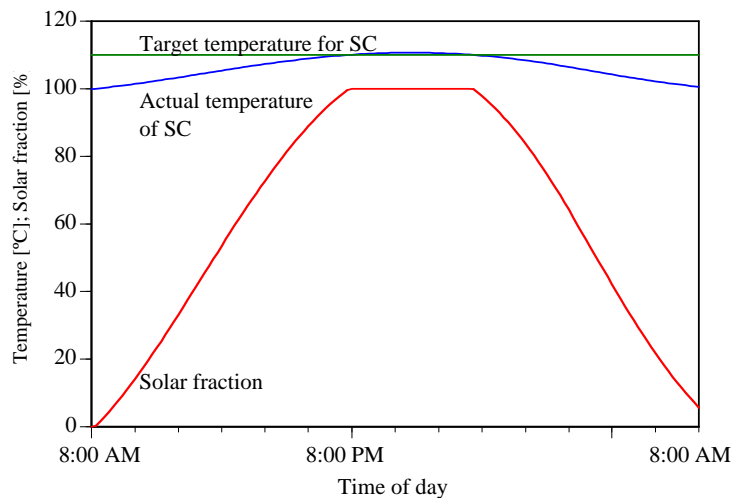


Figure 10. Solar fraction and optimum solar fraction area

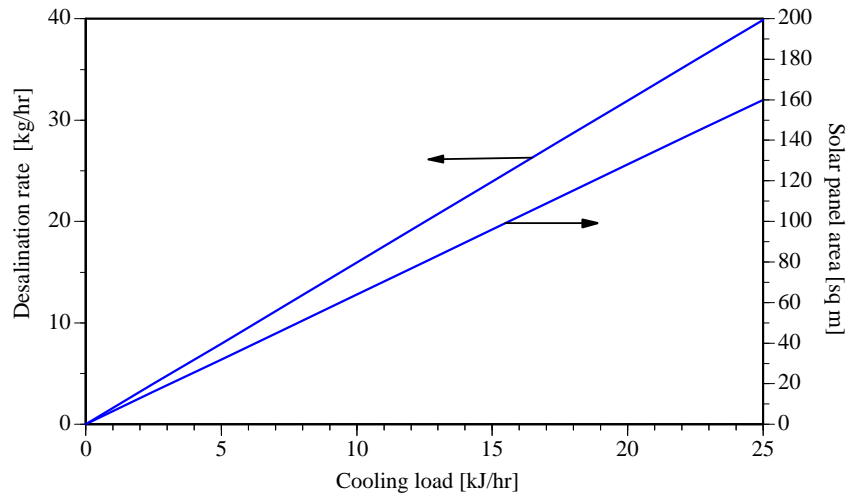


Figure 11. Desalination rates at different cooling rates and solar panel areas

3.1.4 Energy requirements

Apart from the solar energy, the proposed system requires additional mechanical energy to drive the pumps and additional heat energy for the generator to drive the ARS during non-sunlight hours. Simulation results show that the additional mechanical energy requirement is 16 kJ/kg of product plus auxiliary heat energy of 192 kJ/kg of product, totaling to a specific energy requirement of 208 kJ/kg. In comparison, a typical multi-stage flash distillation process requires mechanical energy of 44 kJ/kg of product plus thermal energy of 294 kJ/kg of product, totaling to a specific energy requirement of 338 kJ/kg (Kalogirou, 1997, 2005). Based on simulation results, the proposed process can be an energy efficient and sustainable alternative for desalination.

3.1.5 Brine withdrawal vs. system performance

The brine withdrawal rate is the primary control variable in the proposed system. It has positive as well as negative impacts on the performance of the system. At low withdrawal rates, salts build up in the EC, and evaporation rates decrease. High salt levels also reduce the enthalpy of saline water that can further reduce evaporation (Keren et al., 1993). For example, when salinity increases by 1%, evaporation is also reduced by about the same percentage. Even though better salt removal can be achieved with higher withdrawal rates, large amounts of sensible heat are also simultaneously removed from the EC, resulting in decline of EC temperature. Simulation results presented in Figure 12 show that both EC temperature and the desalination efficiency decline with an increasing withdrawal rate. For example, the desalination efficiency dropped from 90.5% to 80% when the withdrawal rate increased from 2.5 kg/hr to 25 kg/hr.

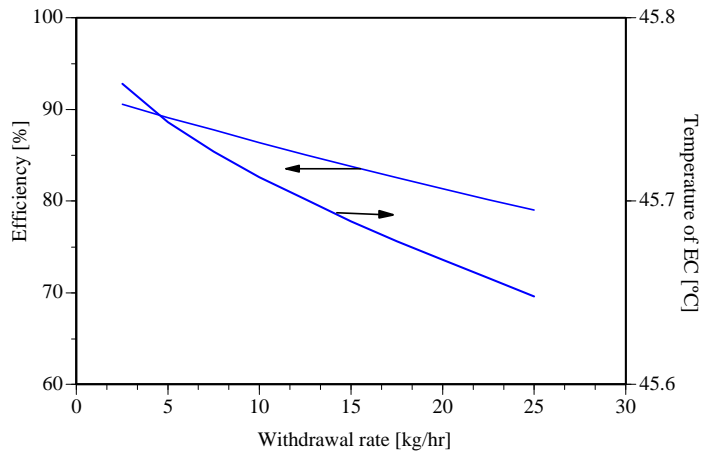


Figure 12. Relationship between withdrawal rate, efficiency and temperature of EC

3.2 Desalination driven by solar photovoltaic/battery system

In this analysis, two configurations for utilizing solar energy were considered: (a) a low-cost system using direct solar energy in the evaporation chamber (EC); and (b) a high-efficiency system using solar photovoltaic (PV) panels. In configuration (a), the EC doubles as a solar still to harvest solar energy during sunlight hours to provide the heat for phase change in the EC. In configuration (b), PV panels harvest solar energy during sunlight hours to charge a battery bank via a charge controller, which in turn, powered a DC heater to heat the EC to maintain it at the set temperature throughout the day. A schematic of configuration (b) is shown in Figure 13.

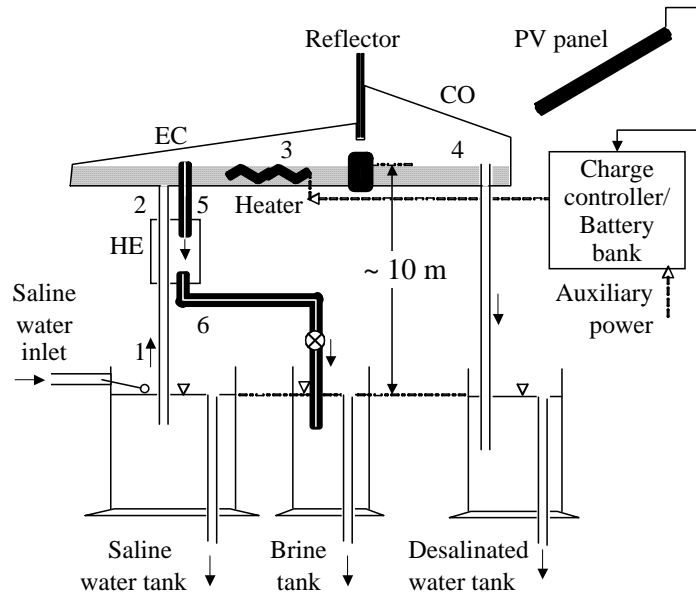


Figure 13. Schematic of the configuration (b): use of solar PV panel/battery bank

Theoretical modeling of these two configurations have been detailed elsewhere (Gude, 2007). Results from prototype scale demonstration of the two configurations are presented below.

3.2.1 Using direct solar energy- Configuration (a)

Initially, configuration (a) was simulated with the following parameters: solar energy incident on evaporation chamber (SEC) area of 1 m^2 ; water depth in the EC of 0.05 m ; and the reference temperature of 25°C . Based on model simulations, configuration A could produce up to 5.25 L/d of freshwater, which is more than twice the productivity of a flat basin solar still of comparable area under comparable solar insolation. This advantage over the solar still is due to the lower evaporation temperature whereby significant energy need for the sensible heat has been averted. Desalination efficiencies of 60-70% could be achieved by this configuration.

The experimental prototype system had an evaporation chamber area of 0.2 m^2 . Since the evaporation rate is a factor of area at given temperatures and pressures, the experimental results from this system are extrapolated to an evaporation area of 1 m^2 to enable comparisons between the experimental results and theoretical simulations. Experimental data from a typical run starting from a “cold start” are shown here to demonstrate the adequacy of the model presented earlier. Figure 14 compares the temperature of the EC predicted by the model against the measured temperature and the ambient temperature in configuration (a). During this test, the solar insolation reached a peak of $1,150 \text{ kJ/hr-m}^2$ over the 8-hour photoperiod. The maximum ambient temperature recorded was 36°C and the maximum temperature of the EC was 52.75°C . The predicted maximum temperature was 52°C . As shown in Figure 14, EC temperature declined after the sunlight period, and approached ambient temperature after sunset. The correlation between the predicted and measured EC temperature was satisfactory with $r^2 = 0.943$, $F = 2358.2$, $p < 0.001$.

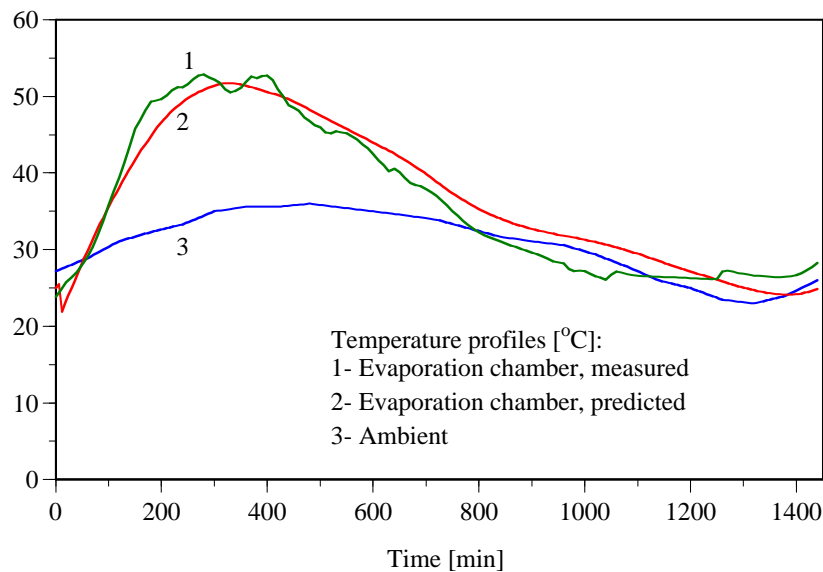


Figure 14. Typical temperature profiles in configuration (a) over one-day period

The predicted distillate volume during the above test is compared against the measured distillate volume in Figure 15. Cumulative volume predicted by the model for a 24-hr period was 5.25 L/day-m^2 while the measured value was 4.95 L/day-m^2 . The difference (of 5.5%) in the cumulative distillate volume is mainly due to the assumption that the entire volume of the vapor distilled on the freshwater side whereas, during the test it was observed that some of the vapor

condensed on the roof of the evaporator and trickled back to the evaporation chamber. Correlation between the predicted and measured distillate volume as a function of time was strong, with $r^2 = 0.988$, $F = 11,839.4$, $p < 0.001$.

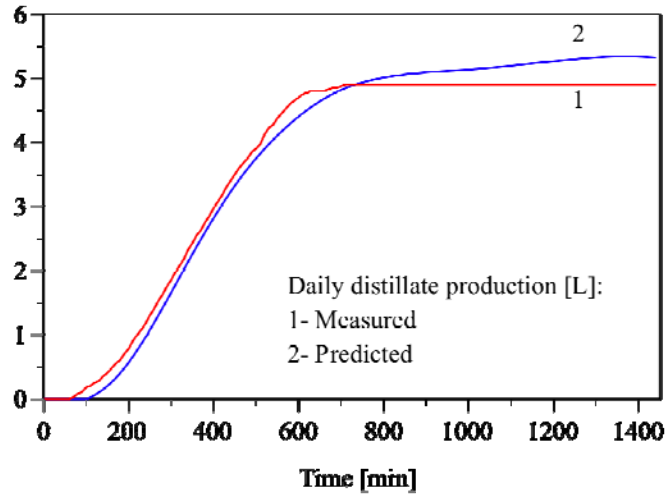


Figure 15. Daily distillate production in configuration (a): Measured vs. predicted

The process efficiency as a function of time predicted by the model is compared in Figure 16 against the efficiency calculated using the measured distillate volume. The predicted efficiency averaged 64% while the observed efficiency averaged 61% over this test period. Correlation between the predicted and measured efficiency was strong, with $r^2 = 0.985$, $F = 538.7$, $p < 0.001$.

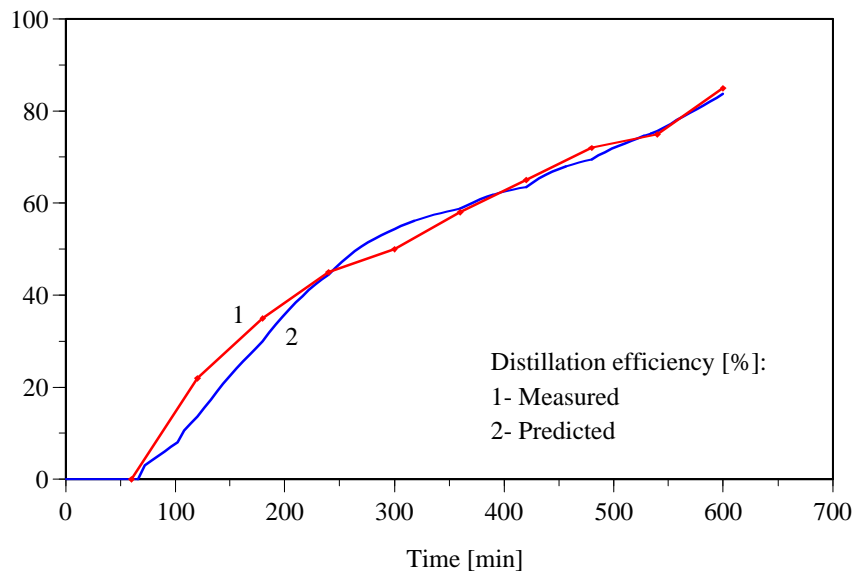


Figure 16. Distillation efficiency in configuration (a): Measured vs. predicted

The above results demonstrate the feasibility of the proposed concept in maintaining the near vacuum pressure in the EC and maintaining continuous flow of the fluids without any mechanical energy input. However, the yield and the efficiency of this system declined when there was no incident solar energy. The performance of configuration (a) was improved slightly when a reflector was installed to increase the incident energy. Figure 17 compares the distillate production rate as a function of time with and without a reflector. During the tests with the reflector, average cumulative production of 7.5 L/day-m² was obtained over 24 hrs. The increased production is due to higher energy input as well as to the slightly longer period of production because of the sensible heat stored in the EC.

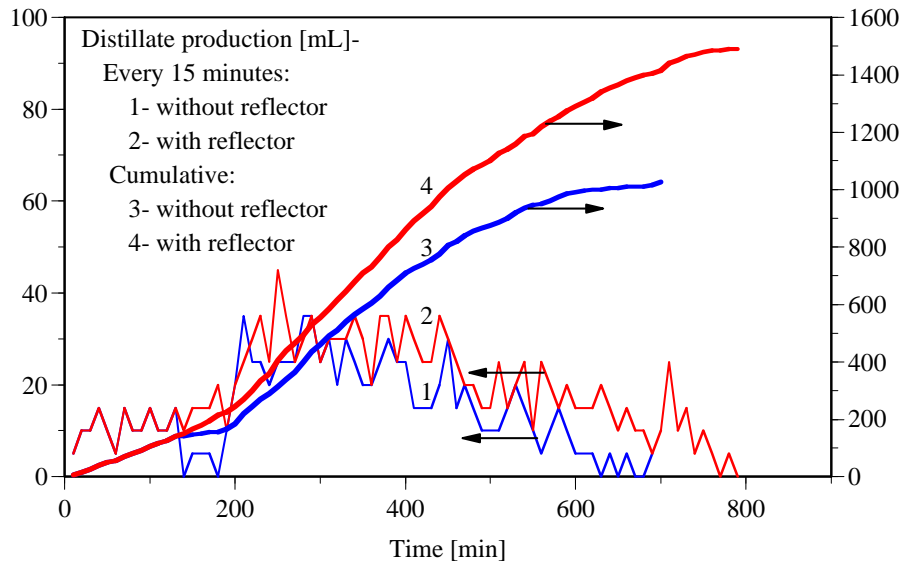


Figure 17. Distillate production with and without a reflector in configuration (a)

3.2.2 Using PV panel and direct solar energy configuration (b)

The limitation of configuration (a) was overcome by using a PV panel/battery bank to heat the EC during non-sunlight hours. In these experiments, a standard PV panel of area 6 m² rated at 185W (Sharp NT-S5E1U) was used to charge a 12-V battery bank, which provided power to a thermostatically controlled 12-V DC heating coil installed in the EC. The efficiency of the PV modules is 14%.

The energy flows during a typical test under this configuration are shown in Figure 18: the incident solar insolation in Figure 18a; the energy produced by the PV panel in Figure 18b; the energy flow to/from the batteries in Figure 18c; and the energy provided to the EC in Figure 18d.

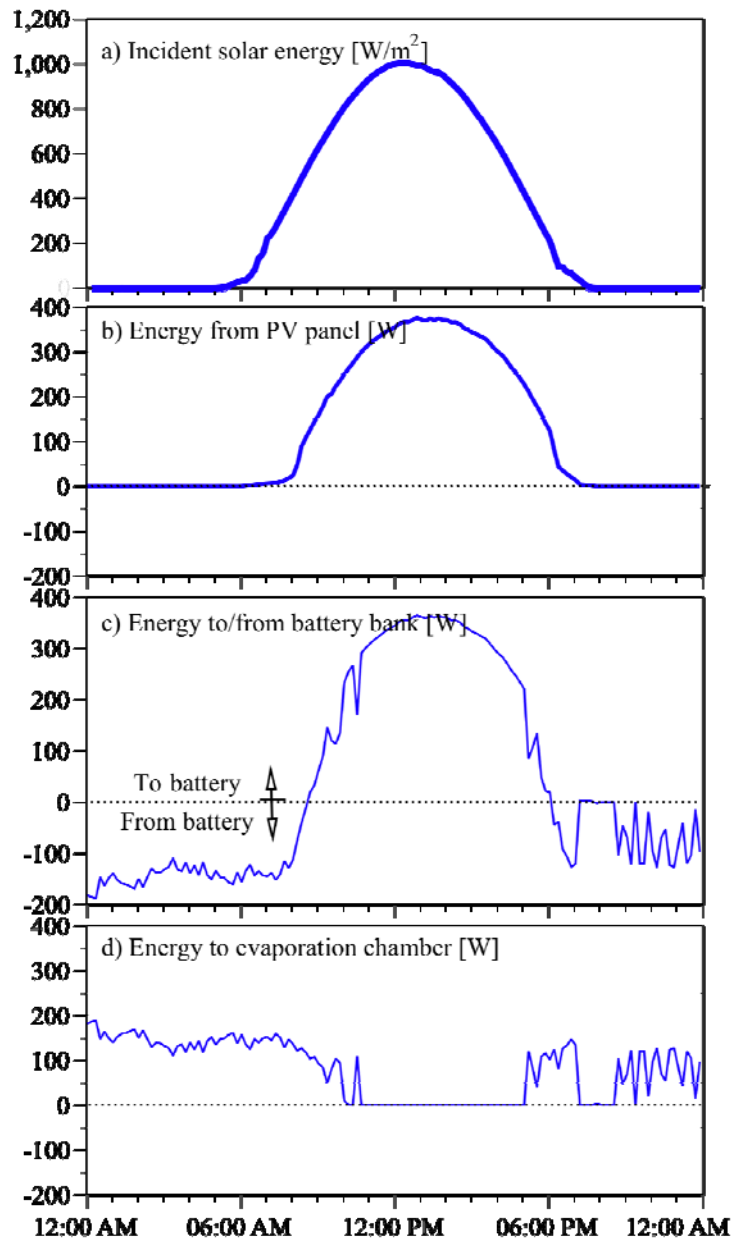


Figure 18. Energy flows in configuration (b) over a typical one-day period

The temperature profiles during a typical test under this configuration are shown in Figure 19. Photovoltaic energy generated during the day was sufficient to produce freshwater of 4-5 L/d-m² during non-sunlight hours. Specific energy required for this process to produce 1 kg of freshwater was 2926 kJ. Freshwater production rates up to 10 L/d-m² have been obtained from this configuration over 24 hours, by maintaining the evaporation temperature nearly constant at the set value throughout the 24-hour period as shown in Figure 19.

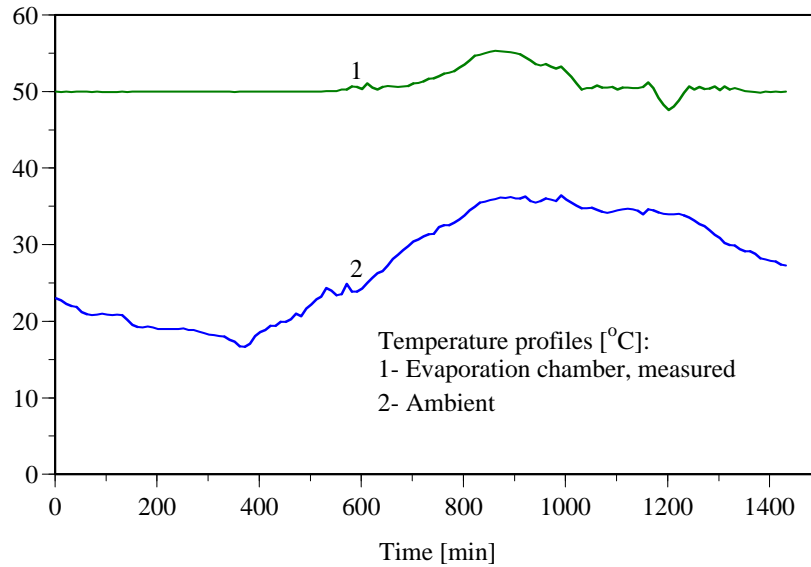


Figure 19. Temperature profiles in configuration (b) with PV/battery

Comparing the temperature profile for configuration (a) with that for configuration (b), the benefit of adding the PV/battery system is obvious. However, it has to be noted that the performance of configuration (b) is limited in this case by the evaporation area rather than the PV panel area. In fact, the PV panel used in this study was oversized, and was able to provide more energy than what is required for evaporation, as shown in Figure 20.

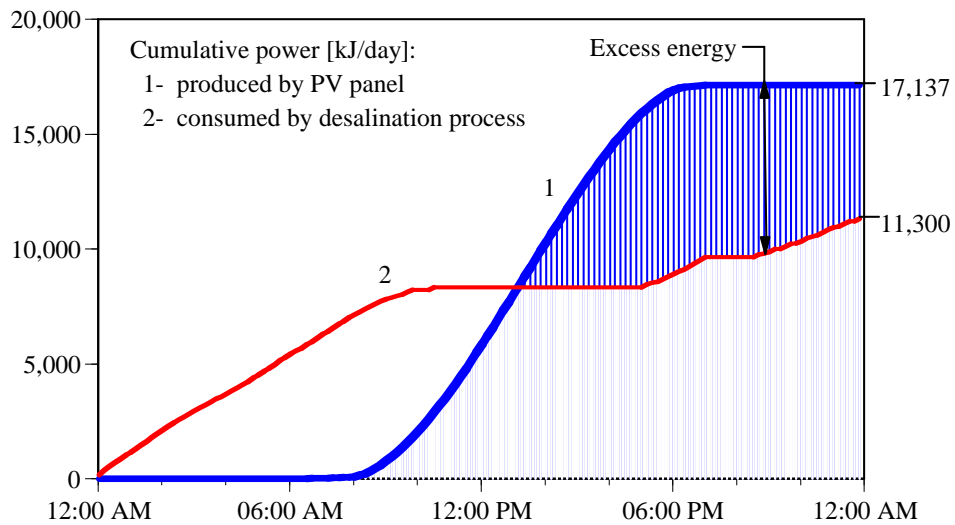


Figure 20. Energy produced, energy consumed, and excess energy

Freshwater production as a function of time in configuration (b) is shown in Figure 21. Comparing the production in configuration (a) (Figure 15) with that in configuration (b) (Figure 21), the benefit of adding the PV/battery system in extending the desalination period is clear.

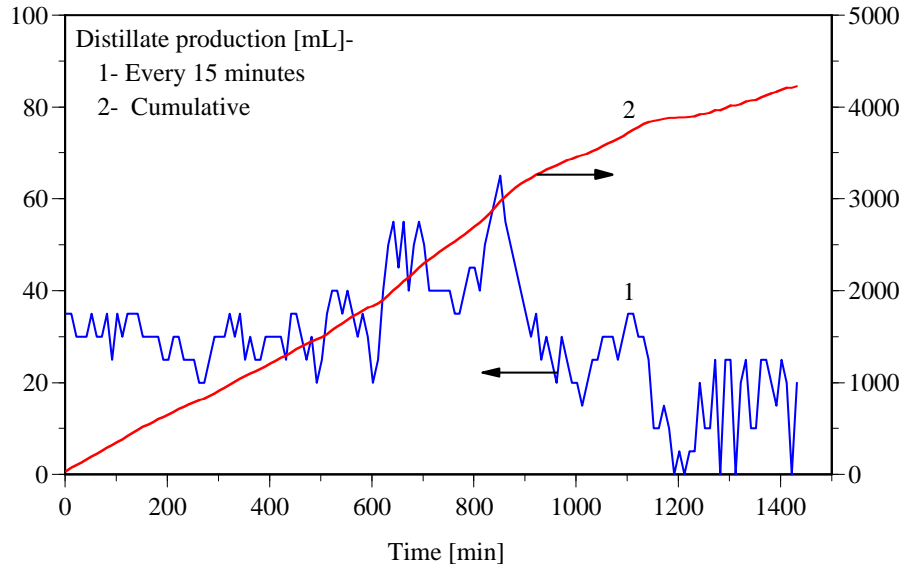


Figure 21. Distillate production in configuration (b) with PV/battery

Grid energy requirements for the proposed process are compared with the following commonly used desalination processes in Table II (Kalogirou, 2005): multi-stage flash distillation (MSF); multi-effect distillation (MED); mechanical vapor compression (MVC); reverse osmosis (RO); and electro dialysis (ED). The process developed in this study eliminates green house gas emissions by using solar energy for heating as well as fluid transfer while the other processes consume non-renewable energy sources for providing the thermal and mechanical energy requirements with green house gas emissions contributing to global warming. In this comparison, 30% production efficiency for the production of electricity from fossil fuels is considered. The carbon dioxide emissions in Table II are estimated based on the assumption that 1 kW-hr electricity production results in 0.96 kg of CO₂ emissions (Ref. 12).

Table II. Comparison of proposed process with traditional desalination processes

		MSF	MED	MVC	RO	ED	SS	PV
Specific energy [kJ/kg]	Thermal	980	410	0	0	0	0	0
	Mechanical	44	26	192	120	144	3.6	0
	Total	1024	436	192	120	144	3.6	0
CO ₂ emissions [kg CO ₂ /kg H ₂ O]		0.38	0.16	0.07	0.05	0.5	~0	0

MSF- Multi-stage flash distillation; MED- Multieffect distillation; MVC- Mechanical vapor compression; RO- Reverse osmosis; ED- Electro dialysis; SS- Solar still; PV- Photovoltaic, this study. Ref. Kalogirou, 2005.

This system could therefore be most suitable for remote areas without an electrical grid. However, the benefit of utilizing natural vacuum principle to save mechanical energy needs has to be evaluated at a large scale to validate the process feasibility. While the proposed process has lower specific energy requirements compared to other single stage evaporation units, its performance can be further improved by adding multi-effect configuration. The ability of this process to utilize renewable energy sources can minimize greenhouse emissions that contribute to global warming, making this a sustainable process. Recovering waste heat from other processes, such as air-conditioning systems and power plants, to drive this process can significantly improve the overall economies of the combined processes.

3.3 Reclamation from wastewater treatment plant effluent

One set of experiments was conducted to evaluate the feasibility of reclaiming water from the effluent of the Las Cruces Municipal Wastewater Treatment Plant. Water samples from the SWT and FWT were analyzed for standard water quality parameters. Results from this set of tests are summarized in Table III relative to the US Environmental Protection Agency Water Quality Standards for drinking water to demonstrate that this process has the potential to reclaim potable-quality water from the wastewater treatment plant effluent. Removal efficiencies of key contaminants were as follows: > 93% total dissolved solids; >95% nitrates; > 97% ammonia; and > 99.9% coliform bacteria.

Table III. Water quality measures before and after treatment

Water quality measure	WWTP effluent	Product water	US EPA Standards
BOD (mg/L)	9.7	-	
TSS (mg/L)	5.1	< 1	
TDS (mg/L)	727	21	500
Nitrates/nitrites(mg/L)	2.4	< 0.1	1
NH ₃ (mg/L)	23.2	< 0.5	
Chlorides (mg/L)	0	0	4
Coliform (cfu/100)	77	< 1	0
pH	7.1	7.1	6.5-8.5

4.0 Conclusions

A new, low-temperature phase-change desalination process suitable for utilizing low-grade heat sources was developed and demonstrated in this study. This study included theoretical analysis, simulation, and experimental validation of the proposed system at prototype scale. Based on the theoretical analyses, this system has the potential to be driven by waste heat rejected by an absorption refrigeration system (ARS) or solar energy. Based on the theoretical analysis, the following results can be expected:

- an ARS system rated at 3.25 kW of cooling can produce 125 L/day of desalinated water.
The net energy input in this case was 208 kJ/kg of freshwater, which is 60% of the energy required by a conventional multi-stage distillation process.
- a solar collector of area 1 m² can produce 8 L/day of desalinated water.
- a photovoltaic/thermal collector unit of area of 25 m² can produce 200 L/day of desalinated water and simultaneously produce 21 kW-hr/day of electrical power as well.

Experimental studies were conducted to validate the process model developed in this project. The feasibility of running the process solely on solar energy, without any reliance on grid power was demonstrated. Based on experimental results, the following conclusions are made:

- a PV module of area 6 m² with an evaporation area of 1 m² can produce 12 L/day of desalinated water, without any energy input from the grid.
- water quality analysis of the product water exceeded the US EPA drinking water standards.

While the research under this grant validated the technical feasibility of the proposed process, further research and long-term testing at higher flow rates need to be undertaken to demonstrate the practical viability and develop data for economic and life cycle analysis of the process. One of the issues to be addressed is the accumulation of non-condensable gases in the evaporation chamber. An automatic pressure venting system may have to be incorporated in such cases. The mathematical models developed in this research could be used for scale-up and process optimization. Further improvements in yield and energy efficiency can be achieved by expanding this system to two or three stage configuration.

5.0 Acknowledgements

This project was executed almost entirely by Veera Gnaneswar Gude, who earned a PhD degree at NMSU based on his theoretical and experimental work on this project, that has resulted in four journal publications, seven International conference presentations, and a patent application. His dedication, hard work, and total commitment toward the timely completion of the project are appreciated very much. Valuable technical support provided by Andy Rosenthal and Corey Asbill of the Institute of Energy & Environment at NMSU and equipment support from Dr. Craig Ricketts of the Engineering Technology Department at NMSU are acknowledged. Assistance in fabricating the prototype system by undergraduate Robert Payne of the Engineering Technology Department is also acknowledged. Funding provided by NM Water Resources Research Institute for undertaking this study and partially supporting two graduate students is gratefully acknowledged.

6.0 References

- Al-Kharabsheh, S.; and Goswami, D.Y., Analysis of an innovative water desalination system using low-grade solar heat, *Desalination*, 2003, 156, 323–332.
- Al-Kharabsheh, S.; and Goswami, D.Y., Experimental study of an innovative solar water desalination system utilizing a passive vacuum technique, *Sol. Energy*, 2003, 75, 395–401.
- Bemporad, G.A. Basic hydrodynamic aspects of a solar energy based desalination process, *Sol. Energy*, 1995, 54, 2, 125–134.
- Gude, V.G.; and Nirmalakhandan, N., Desalination using low-grade heat sources, *ASCE J Energy Engrg.*, 2008, 134, 95-101.
- Gude, V.G.; and Nirmalakhandan, N., Combined desalination and solar-assisted air-conditioning system, *Energy Conv. & Management*, 49, 3326-3330, 2008.
- Gude V.G.; and Nirmalakhandan, N., Desalination at low temperatures and low pressures, *Desalination*, 2009, 244, 239-247.
- Gude, V.G., PhD Dissertation, New Mexico State University, Las Cruces, NM, USA 2007.
- Gustavo K.; and Fredi L. Low-temperature distillation processes in single- and dual purpose plants. *Desalination*, 2001;136:189–97.
- http://www.eia.doe.gov/cneaf/electricity/page/co2_report/co2report.html#electric2000
- Kalogirou, S.A., Economic analysis of a solar assisted desalination system, *Renewable Energy*, 1997, 124, 351-367.
- Kalogirou, S.A., Seawater desalination using renewable energy sources. *Prog. Energy Combust. Sci.*, 2005, 31, 242–281.
- Keren Y., Rubin H., Atkinson J., Priven M., and Bemporad G.A. Theoretical and experimental comparison of conventional and advanced solar pond performance. *Sol. Energy* 1993; 51:255–70.